Published in final edited form as:
Photochem Photobiol. 2009 ; 85(5): 1177–1181. doi:10.1111/j.1751-1097.2009.00555.x.

Monitoring Singlet Oxygen and Hydroxyl Radical Formation with Fluorescent Probes During Photodynamic Therapy

Michael Price[1], **John J Reiners**[2], **Ann Marie Santiago**[3], and **David Kessel**[3,*]

[1]Cancer Biology Program, and Karmanos Cancer Institute, Wayne State University School of Medicine, Detroit, MI

[2]Institute of Environmental Health Sciences, Wayne State University, Detroit, MI

[3]Departments of Pharmacology and Medicine, Wayne State University School of Medicine, Detroit, MI

Abstract

Singlet oxygen ($^1O_2$) is the primary oxidant generated in photodynamic therapy (PDT) protocols involving sensitizers resulting in type II reactions. $^1O_2$ can give rise to additional reactive oxygen species (ROS) such as the hydroxyl radical (•OH). The current study was designed to assess 3′-*p*-(aminophenyl) fluorescein (APF) and 3′-*p*-(hydroxyphenyl) fluorescein (HPF) as probes for the detection of $^1O_2$ and •OH under conditions relevant to PDT. Cell-free studies indicated that both APF and HPF were converted to fluorescent products following exposure to $^1O_2$ generated by irradiation of a water-soluble photosensitizing agent (TPPS) and that APF was 35-fold more sensitive than HPF. Using the $^1O_2$ probe singlet oxygen sensor green (SOSG) we confirmed that 1 mM NaN_3 quenched $^1O_2$-induced APF /HPF fluorescence, while 1% DMSO had no effect. APF and HPF also yielded a fluorescent product upon interacting with •OH generated from H_2O_2 via the Fenton reaction in a cell-free system. DMSO quenched the fluorogenic interaction between APF /HPF and •OH at doses as low as 0.02%. Although NaN_3 was expected to quench •OH-induced APF /HPF fluorescence, co-incubating NaN_3 with APF or HPF in the presence of •OH markedly enhanced fluorescence. Cultured L1210 cells that had been photosensitized with benzoporphyhrin derivative exhibited APF fluorescence immediately following irradiation. Approximately 50% of the cellular fluorescence could be suppressed by inclusion of either DMSO or the iron-chelator desferroxamine. Combining the latter two agents did not enhance suppression. We conclude that APF can be used to monitor the formation of both $^1O_2$ and •OH in cells subjected to PDT if studies are performed in the presence and absence of DMSO, respectively. That portion of the fluorescence quenched by DMSO will represent the contribution of •OH. This procedure could represent a useful means for evaluating formation of both ROS in the context of PDT.

INTRODUCTION

The efficacy of photodynamic therapy (PDT) derives from the initial formation of singlet oxygen ($^1O_2$). In turn, $^1O_2$ can give rise to several other types of reactive oxygen species (ROS) including superoxide anion, hydrogen peroxide, and hydroxyl radical (•OH). The contributions of these various ROS types to the biochemical and morphological changes after PDT are often inferred by the inclusion of ROS type-specific scavengers. What is missing are simple fluorescence-based assays for real-time monitoring of specific types of ROS.

*Corresponding author: dhkessel@med.wayne.edu (David Kessel).

The fluorescent probes, 3′-*p*-(aminophenyl) fluorescein (APF) and 3′-*p*-(hydroxyphenyl) fluorescein (HPF), were synthesized by Setsukinai *et al.* (1) as tools for stable and selective detection of •OH and peroxynitrite. Both probes were reported to be cell-permeable, relatively insensitive to super-oxide anion radical, nitric oxide, $^1O_2$ and alkyl peroxides and free from the auto-oxidation associated with some other probes. However, they differed substantially in their responsiveness to hypochlorite ion (ClO^-). APF was converted to a fluorescent form by ClO^- while HPF was not.

The current studies were initially designed to assess the potential usefulness of HPF and APF as cell-permeable probes for the detection of •OH during PDT. Initial studies carried out in a cell-free system using generators of •OH or $^1O_2$ revealed that APF, and to a lesser extent HPF, were converted to fluorescent products by either ROS. Inclusion of DMSO quenched the fluorescence generated by •OH interaction with either probe. In contrast, NaN_3 quenched only the fluorescence generated by interactions with $^1O_2$. In the context of PDT, cultured L1210 leukemia cells that had been sensitized with benzoporphyhrin derivative (BPD) exhibited APF fluorescence within seconds of irradiation. Quenching studies revealed that at least 50% of this fluorescence could be attributed to the generation of •OH. Surprisingly, the amount of DMSO needed for quenching of the •OH-derived fluorescence represented a concentration that is often used as a solvent carrier in biological systems.

We also examined the effects of quenching agents on the fluorogenic detection of $^1O_2$ by singlet oxygen sensor green (SOSG), described in Ref. (2). Effects of two ROS quenchers were also determined: NaN_3 and DMSO. The latter is expected to be specific for •OH (3,4).

MATERIALS AND METHODS

Chemicals

For generation of $^1O_2$, we employed the tetra-sulfonated photosensitizing agent porphine tetra (*p*-phenylsulfonate) (TPPS), purchased from Porphyrin Products, Logan, UT. Solutions (10 mM) were made up in water and stored at 4°C in the dark. The fluorescent probes SOSG, HPF and APF were obtained from Invitrogen as solutions in methanol (SOSG) or dimethyl formamide (APF and HPF). Structures of the latter two agents are shown in Fig. 1. BPD was provided by VWR and dissolved in dimethyl formamide. Other chemicals were purchased from Fisher Scientific Co. and were of the highest obtainable purity.

Fluorescence assay procedures

An SLM 48000 fluorometer, modified by ISS (Champaign, IL), was used for acquisition of fluorescence signals in the “slow kinetic” mode. When APF or HPF were employed, fluorescence emission at 525 nm was measured upon excitation at 492 nm using 2 nm slit widths for both excitation and emission. With SOSG, the corresponding values were 505 and 525 nm, respectively.

Studies involving a cell-free system were carried out in 1 × 1 × 3 cm glass cuvettes maintained at a temperature of 20°C by a Peltier system, and stirred constantly. When a diode laser was used for the photodynamic generation of $^1O_2$, the influence of stray light from the laser was minimized by insertion of a 500 ± 35 nm interference filter into the emission beam. In all experiments, the fluorescent probes were present at 3 μM concentrations.

Singlet oxygen formation

Singlet oxygen was generated by a photodynamic reaction (5) in 3 mL of 100 mM phosphate buffer pH 7.0, H_2O or D_2O, along with 10 μM TPPS. A 400 μm fiber bundle was used to transfer 649 nm light from a laser diode to the top surface of the cuvette, using a power density of 1

mW cm^{-2}. This permitted irradiation during the acquisition of a fluorescence signal in real time. The laser was activated immediately before the beginning of fluorescence acquisition, with data points acquired at 4 s intervals over 180 s. The change in fluorescence as a function of time was linear for at least 120 s.

Formation of hydroxyl radical

This ROS was generated by the Fenton reaction (6) using a mixture containing 100 mM phosphate buffer pH 7,0, 0.3 mM $Fe(NH_4)_2(SO_4)_2$ (FAS) and 0.3 mM H_2O_2. Addition of H_2O_2 resulted in a rapid increase in fluorescence. We report the steady-state fluorescence signal *minus* the base-line signal obtained before addition of H_2O_2 (Table 1).

Quenching studies

Fluorogenic interactions involving $^1O_2$ and $^{\bullet}OH$ and fluorescent probes were assessed in the absence *vs* presence of inhibitors (NaN_3 or DMSO) using SOSG, APF or HPF in systems described above. Data are reported in Fig. 2 and Fig 3 and in Table 1.

Photodynamic studies in cell culture

Procedures for these studies and the subsequent morphometric analysis of images have been described (7). Murine leukemia L1210 cells were incubated with 2 μM BPD + 3 μM APF for 30 min at 37°C. In replicate tubes DMSO (1%), 100 μM desferroxamine (DFO) or both reagents were added. The cells were then collected by centrifugation (100 ***g***, 30 s), resuspended in fresh medium and irradiated. The light dose was 67.5 mJ cm^{-2} at 690 ± 5 nm, as determined with a ScienTech H10T radiometer. This PDT dose was previously found to reduce cell viability to 11 ± 3% of control values, as indicated by clonogenic assays.

After irradiation, cells were collected by centrifugation and examined by fluorescence microscopy using 450–490 nm excitation, and monitoring emission at 520–600 nm. A Nikon Eclipse E600 microscope was used for this purpose, with images acquired by a Photometrics CoolSnap HQ CCD camera operated at −40°C at the highest sensitivity setting. An exposure time of 1000 ms was required to obtain the images shown in Fig. 4. A B2A filter cube was used (excitation = 450–490 nm). The emission was controlled by a high-pass 520 nm filter and an additional 600 nm low-pass filter to screen out fluorescence derived from BPD.

Images of cellular fluorescence were captured using MetaMorph software (Molecular Devices, MDS Analytical Technologies). Average pixel intensities were determined using morphometric analysis.

Morphometric analysis procedure

A thresholding process was first used to select only those portions of the image representing cellular fluorescence. The black background was therefore omitted from the calculations. The average grayscale analysis was then calculated as the summation of the values for each pixel contained in the images of the cells (0 = black, 255 = white). This value was then divided by the total number of pixels constituting cell images, so that an average pixel brightness is represented.

RESULTS AND DISCUSSION

Fluorogenic response of HPF and APF to hydroxyl radicals and quenchers

The effects of $^{\bullet}OH$ on APF and HPF fluorescence are summarized in Table 1. We found APF yielded ~5-fold more fluorescence during $^{\bullet}OH$ formation than did HPF. In Ref. (1), it was reported that APF was more sensitive than HPF by a factor of 1.7. In experiments reported

here, we used FAS rather than the $Fe(ClO_4)_2$ employed in Ref. (1), since we found that the latter salt resulted in formation of a precipitate in phosphate buffer. There was no precipitation when FAS was used as the source of ferrous iron.

In a cell-free system, the fluorogenic reaction of $^{\bullet}OH$ with HPF or APF was quenched ~50% by 0.02% DMSO (vol / vol). A concentration of 0.1% DMSO, often said to be safe for use in biological studies, was found to decrease the fluorogenic response of APF to $^{\bullet}OH$ by >90%. In the presence of 1 mM NaN_3, an unexpected increase in fluorescence was observed (Table 1). Hence, this reagent could not be used in quenching studies.

Determinants of singlet oxygen formation

$^1O_2$ formation was monitored using SOSG (Fig. 2, top). During irradiation of an aqueous solution of TPPS + SOSG, we observed a progressive increase in 525 nm fluorescence that was markedly enhanced in D_2O. This effect is expected since the lifetime of the triplet state is strongly promoted in deuterated solvents (8). The fluorogenic effect of $^1O_2$ on SOSG was slightly promoted by the presence of 100 mM phosphate buffer pH 7.0, compared with water alone.

Quenching studies carried out with SOSG in phosphate buffer (Fig. 2, bottom) showed only a minor effect of 1% (vol / vol) DMSO on $^1O_2$-mediated fluorescence, but a substantial quenching of the fluorogenic reaction by NaN_3.

Fluorogenic responses of HPF and APF to singlet oxygen

Irradiation of an aqueous solution containing APF + TPPS resulted in a fluorogenic response that was enhanced >25-fold in D_2O (Fig. 3). This fluorogenic reaction was greater in phosphate buffer than in water. Additional photodynamic studies carried out in phosphate buffer revealed only a slight quenching of APF fluorescence by 1% DMSO, but a very substantial decrease upon addition of 1 mM NaN_3 (Fig. 3). These characteristics are consistent with the behavior of $^1O_2$ + SOSG shown in Fig. 2.

HPF was substantially less sensitive to $^1O_2$ than APF. In D_2O, the fluorogenic interaction of $^1O_2$ with APF during irradiation proceeded at a ~35-fold greater rate than was observed with HPF (Fig. 3, line designated “HPF D_2O”). These values differ from what was reported in Ref. (1), where HPF was found to be ~50% as responsive to $^1O_2$ as APF. In Ref. (1), the comparison was carried out in phosphate buffer. We used D_2O in our studies to increase the signal-to-noise ratio since the fluorogenic interaction between HPF and $^1O_2$ in H_2O or phosphate buffer was barely detectable (not shown). Since DMSO is known to quench $^{\bullet}OH$ but not $^1O_2$ (3,4), these data show that APF and HPF can detect $^1O_2$ formed during PDT.

ROS detection in cell cultures

TPPS was useful for studies in an aqueous cell-free system since it does not aggregate in aqueous solution. In order to carry out studies in cell culture, we selected a more hydrophobic agent, BPD, that was readily accumulated by L1210 cells. To determine the potential usefulness of APF in PDT studies, we incubated L1210 cells with APF and BPD, followed by irradiation to achieve an LD_{90} PDT dose. The fluorescence images shown in Fig. 4 were all obtained at the same camera settings. For this study, a 600 nm low-pass filter was placed in the emission pathway to eliminate fluorescence from the photosensitizing agent. In nonirradiated cultures, only weak APF fluorescence could be detected (panel A).

Irradiation of photosensitized cells resulted in substantial APF-derived fluorescence (panel B). Addition of either 1% DMSO or the iron-chelator DFO resulted in loss of fluorescence (panels C and D). Adding both reagents simultaneously did not significantly increase this quenching

(panel E). A morphometric analysis of the results is summarized in Table 2. DFO is known to quench hydroxyl radical formation generated via the Fenton reaction (9–11). Analysis of fluorescence intensities indicates ~50% of the total APF fluorescence was derived from processes quenched equally by DFO or DMSO, presumably representing $^{\bullet}OH$ (Table 2). Adding both reagents did not further promote fluorescence quenching, consistent with the proposal that the signal abolished by DMSO represents $^{\bullet}OH$. Even when the DMSO concentration was reduced to 0.1%, some quenching of the portion of the fluorescent signal attributed to $^{\bullet}OH$ was observed (Fig. 4, panel F). This was readily quantified by the morphometric analysis technique (Table 2).

We also examined the possibility that HPF might be useful in monitoring $^{\bullet}OH$ formation during irradiation of photosensitized cells. Unfortunately, the interaction between $^{\bullet}OH$ and HPF produces only 20% of the fluorescence intensity observed with APF (Table 1). As a result, detection of a fluorescent signal from HPF after an LD_{90} PDT dose would require a 5000 ms exposure. This was found to be associated with substantial photobleaching of the probe (not shown). Since SOSG cannot be used with intact cells because of its inability to penetrate the cell membrane (1) and the often-used probe 2,7-dichlorofluorescein diacetate is readily auto-oxidized (1), we propose that APF or HPF should be useful for “on-line” monitoring of $^1O_2$ formation, in the presence of DMSO to suppress $^{\bullet}OH$ formation.

CONCLUSIONS

These studies show that in the context of PDT, where a very substantial concentration of $^1O_2$ is formed, APF can be a useful cell-permeable probe for detecting formation of this ROS. Moreover, the selective use of DMSO can provide a means for assessing $^{\bullet}OH$ formation.

APF and HPF are often used as fluorescent probes for the detection of hydroxyl radical hypochlorite (12–14). It was initially reported (1) that these probes were relatively insensitive to $^1O_2$ (1). However, our studies indicate that, under conditions associated with PDT, fluorogenic interactions with $^1O_2$ can be significant, with APF substantially more sensitive to $^1O_2$ than HPF. Since maximum sensitivity to $^{\bullet}OH$ was an important consideration, we employed the more responsive probe APF to determine whether $^{\bullet}OH$ could be detected in the presence of $^1O_2$ in cell culture.

Quenching studies indicated that 0.1% DMSO could suppress >90% of the APF fluorescence derived from $^{\bullet}OH$ (Table 1) without affecting the signal derived from $^1O_2$ (Fig. 3). The ability of concentrations of DMSO as low as 0.02% to quench $^{\bullet}OH$ in a cell-free system indicates that this solvent is best omitted from any study designed to assess formation or effects of this ROS. A study with murine leukemia L1210 cells and the photosensitizing agent BPD revealed that the use of APF in the presence *vs* absence of DMSO is a feasible approach for monitoring $^{\bullet}OH$ formation during irradiation of photosensitized cells (Fig. 4). While HPF would appear to be a better probe because of its decreased response to $^1O_2$, this advantage is offset by its much weaker response to $^{\bullet}OH$. Use of HPF requires a sufficiently long exposure time such that there is photobleaching of the probe, and a nonlinear result. In the presence of DMSO, we propose that APF may be a useful means for assessing $^1O_2$ formation during PDT. SOSG, while a useful probe for $^1O_2$, is impermeable to cells (2).

In Ref. (1) it was calculated that APF is ~130-fold more sensitive to $^{\bullet}OH$ than to $^1O_2$. If we assume this ratio is pertinent to the present studies, we can estimate the relative contribution of each ROS to the fluorogenic response by APF in cell culture. Data shown in Table 2 indicate that approximately half of the fluorescence of APF, after an LD_{90} PDT dose, can be quenched by DMSO or DFO. Based on the ratio from Ref. (1), this translates into ~130 molecules of $^1O_2$ formed for each molecule of $^{\bullet}OH$.

It has been proposed (15) that the conversion of 2-deoxy-D-ribose to products that react with thiobarbituric acid could be an additional test for •OH formation during PDT, as could a fluorescence assay involving derivatives of terephthalate (16). These and other potential methods for assessing •OH formation during PDT need to be evaluated with regard to the potential for interactions with $^1O_2$.

Acknowledgement

These studies were supported by grant CA 23378 from the National Cancer Institute, NIH.

REFERENCES

1. Setsukinai K, Urano Y, Kakinuma K, Majima HJ, Nagano T. Development of novel fluorescence probes that can reliably detect reactive oxygen species and distinguish specific species. J. Biol. Chem 2003;278:3170–3175. [PubMed: 12419811]
2. Flors C, Fryer MJ, Waring J, Reeder B, Bechtold U, Mullineaux PM, Nonell S, Wilson MT, Baker NR. Imaging the production of singlet oxygen in vivo using a new fluorescent sensor, Singlet Oxygen Sensor Green. J. Exp. Bot 2006;57:1725–1734. [PubMed: 16595576]
3. Wei H, Cai Q, Rahn R, Zhang X. Singlet oxygen involvement in ultraviolet (254 nm) radiation-induced formation of 8-hydroxy-deoxyguanosine in DNA. Free Radic. Biol. Med 1997;23:148–154. [PubMed: 9165307]
4. Wasil M, Halliwell B, Grootveld M, Moorhouse CP, Hutchison CD, Baum H. The specificity of thiourea, dimethylthiourea and dimethyl sulphoxide as scavengers of hydroxyl radicals. Their protection of alpha 1-antiproteinase against inactivation by hypochlorous acid. Biochem. J 1987;243:867–870. [PubMed: 2821995]
5. Weishaupt KR, Gomer CJ, Dougherty TJ. Identification of singlet oxygen as the cytotoxic agent in photoinactivation of a murine tumor. Cancer Res 1976;36:2326–2329. [PubMed: 1277137]
6. Fenton HJH. Oxidation of tartaric acid in presence of iron. J. Chem. Soc. Trans 1894;65:899–911.
7. Kessel D, Reiners JJ Jr. Apoptosis and autophagy after mitochondrial or endoplasmic reticulum photodamage. Photochem. Photobiol 2007;83:1024–1028. [PubMed: 17880495]
8. Gorman, AA.; Rodgers, MAJ. Singlet oxygen. In: Sciano, JC., editor. The Handbook of Organic Photochemistry. Vol. Volume 2. Boca Raton, FL: CRC Press; 1989. p. 229-247.
9. Hoe S, Rowley DA, Halliwell B. Reactions of ferrioxamine and desferrioxamine with the hydroxyl radical. Chem. Biol. Interact 1982;41:75–81. [PubMed: 6896472]
10. Faurschou A, Gniadecki R. TNF-alpha stimulates Akt by a distinct ∀PKC-dependent pathway in premalignant keratinocytes. Exp. Dermatol 2008;17:992–997. [PubMed: 18557926]
11. Entman ML, Youker K, Shoji T, Kukielka G, Shappell SB, Taylor AA, Smith CW. Neutrophil induced oxidative injury of cardiac myocytes. A compartmented system requiring CD11b / CD18-ICAM-1 adherence. J. Clin. Invest 1992;90:1335–1345. [PubMed: 1357003]
12. Franco R, Panayiotidis MI, Cidlowski JA. Glutathione depletion is necessary for apoptosis in lymphoid cells independent of reactive oxygen species formation. J. Biol. Chem 2007;282:30452–30465. [PubMed: 17724027]
13. Sumitomo K, Shishido N, Aizawa H, Hasebe N, Kikuchi K, Nakamura M. Effects of MCI-186 upon neutrophil-derived active oxygens. Redox. Rep 2007;12:189–194. [PubMed: 17705989]
14. Indo HP, Davidson M, Yen HC, Suenaga S, Tomita K, Nishii T, Higuchi M, Koga Y, Ozawa T, Majima HJ. Evidence of ROS generation by mitochondria in cells with impaired electron transport chain and mitochondrial DNA damage. Mitochondrion 2007;7:106–118. [PubMed: 17307400]
15. Chekulayeva LV, Shevchuk IN, Chekulayev VA, Ilmarinen K. Hydrogen peroxide, superoxide, and hydroxyl radicals are involved in the phototoxic action of hematoporphyrin derivative against tumor cells. J. Environ. Pathol. Toxicol. Oncol 2006;25:51–77. [PubMed: 16566710]
16. Saran M, Summer KH. Assaying for hydroxyl radicals: hydroxylated terephthalate is a superior fluorescence marker than hydroxylated benzoate. Free Radic. Res 1999;31:429–436. [PubMed: 10547187]

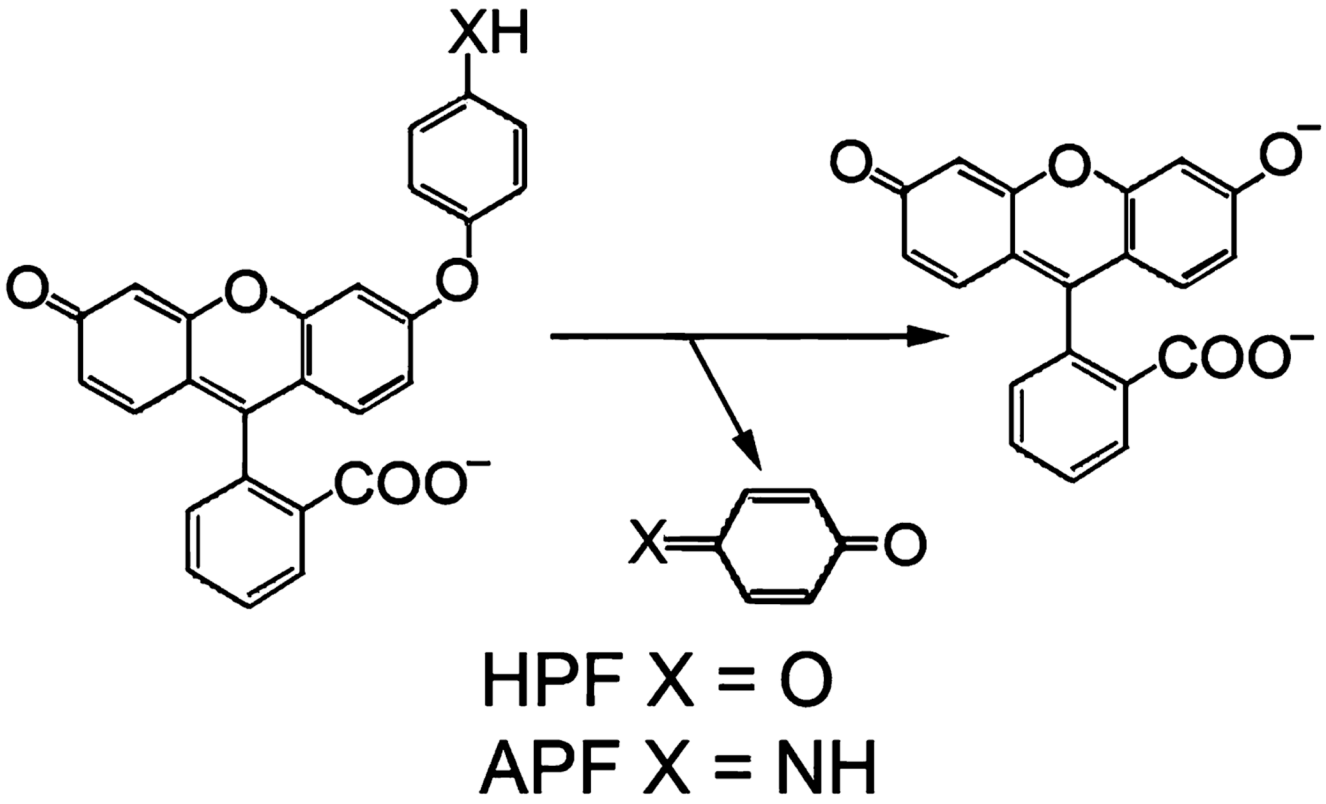

Figure 1.
Structures of HPF and APF and the oxidative reaction that leads to the formation of fluorescein.

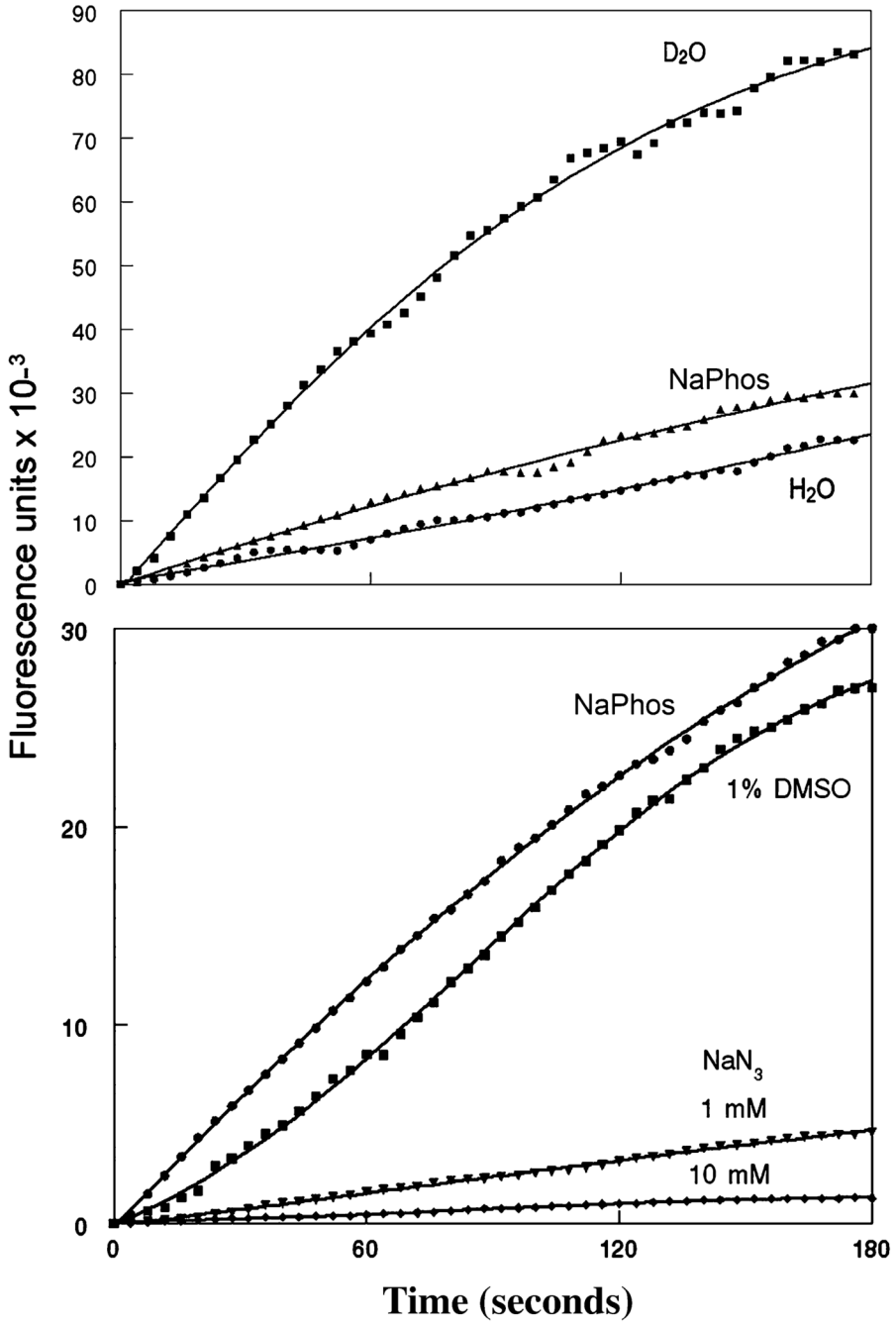

Figure 2.

Top: fluorogenic interactions between 3 μM SOSG and $^1O_2$ during the irradiation at 649 nm of solutions containing 10 μM TPPS. The solvents were D_2O, 100 mM sodium phosphate buffer pH 7.0, or water, using a light flux of 1 mW sq cm^{-1}. Fluorescence was monitored using excitation = 505 nm, emission = 525 nm. Bottom: quenching of fluorescence during irradiation of SOSG + TPPS in phosphate buffer by 1 and 10 m_M sodium NaN_3 and by 1% DMSO.

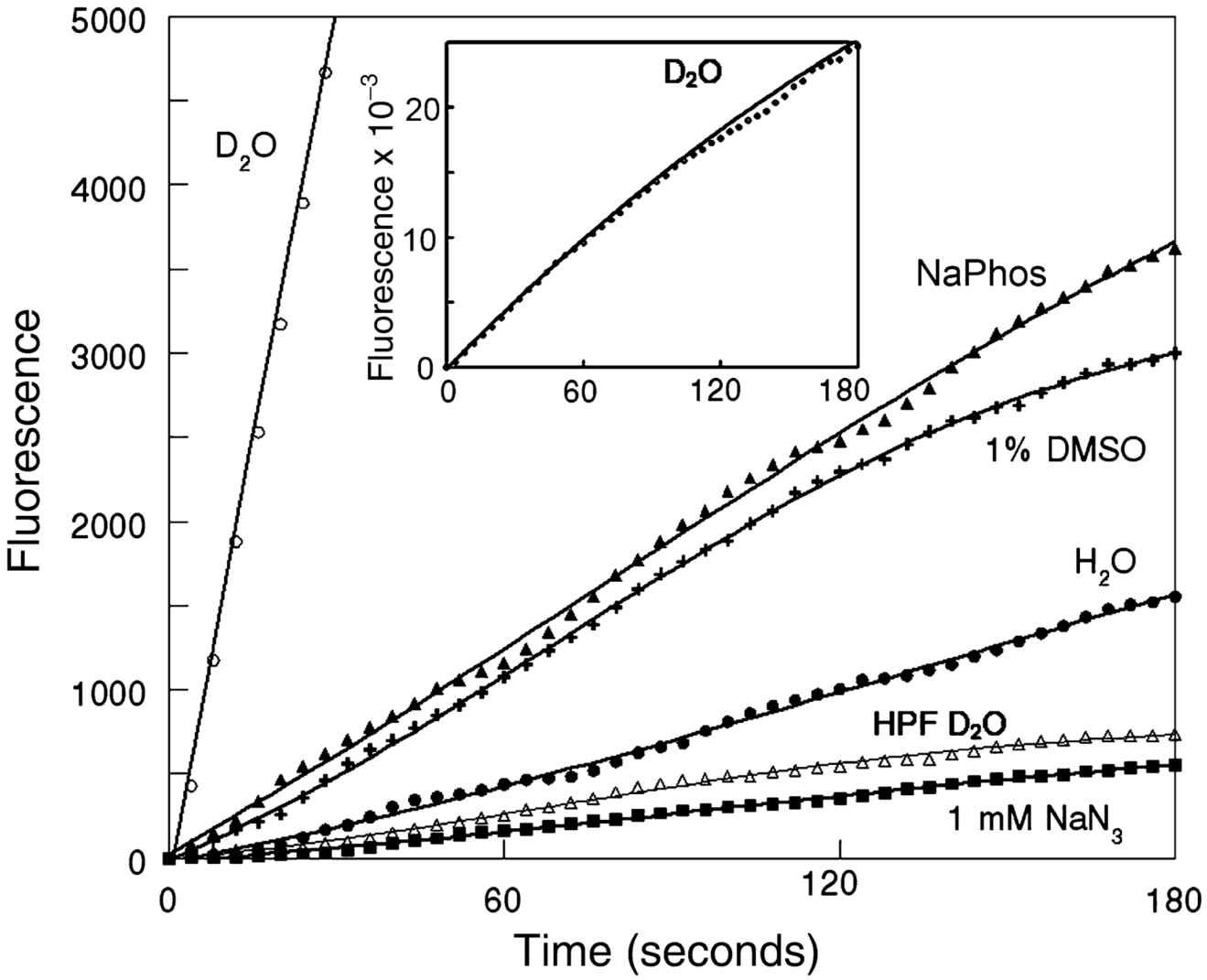

Figure 3.

Fluorogenic interactions of 10 μM TPPS + APF in D_2O, phosphate buffer or water during irradiation (649 nm). Also shown are effects of 1 mM NaN_3 and 1% DMSO in phosphate buffer. For comparison, the fluorogenic reaction with HPF in D_2O is also shown. Inset: the fluorogenic interaction during irradiation between TPPS + APF over 180 s in D_2O. For all studies, excitation = 492 nm, emission = 525 nm.

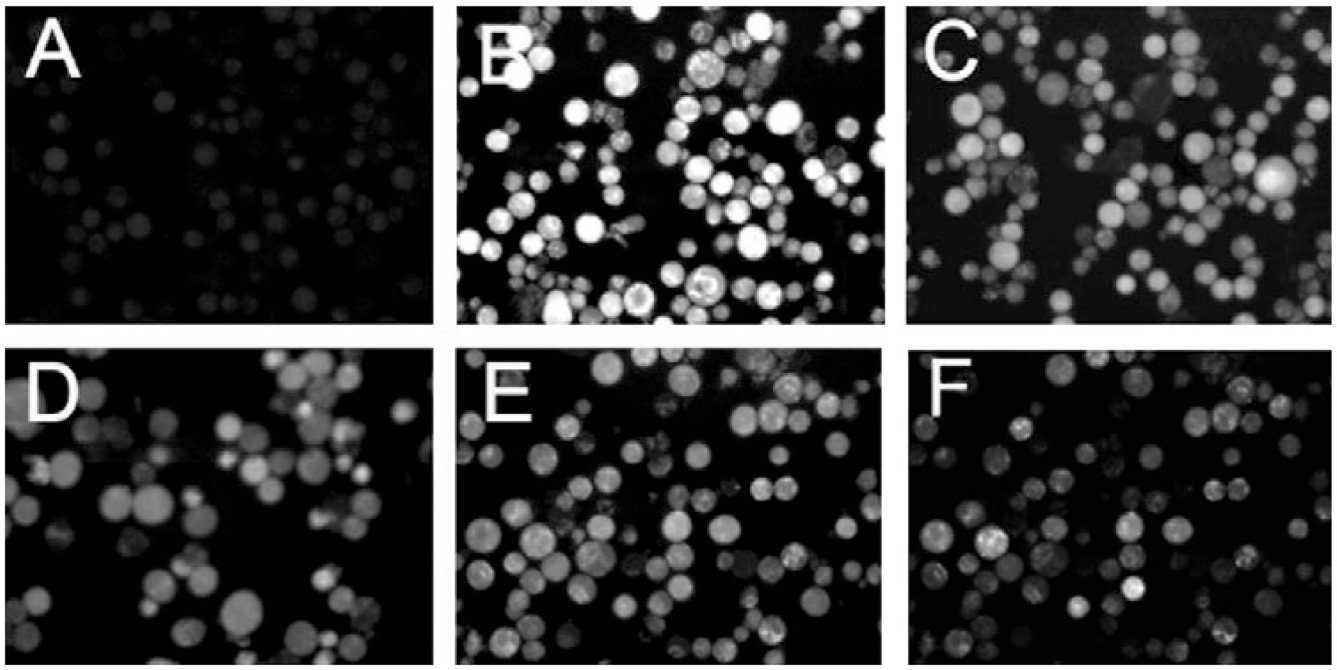

Figure 4.
Fluorescence images of APF fluorescence using L1210 cells photosensitized by BPD. A = dark control (no irradiation), B–E = irradiated cells, B = no additions, C = 1% DMSO, D = 100 μM DFO, E = 1% DMSO + 100 μM DFO, F = 0.1% DMSO. Inhibitors were present during BPD loading, and added back to the culture medium during irradiation.

Table 1

Fluorogenic response to •OH in a cell-free system.

System	Fluorescence units	
	APF	HPF
$Fe^{2+} + H_2O_2$	6117 ± 420	1339 ± 75
$Fe^{2+} + H_2O_2$ + 1 mM NaN_3	28560 ± 175	31295 ± 203
$Fe^{2+} + H_2O_2$ + 1% DMSO	170 ± 18	37 ± 11
$Fe^{2+} + H_2O_2$ + 0.1% DMSO	680 ± 35	148 ± 36
$Fe^{2+} + H_2O_2$ + 0.02% DMSO	2980 ± 806	630 ± 25

Cuvettes contained 3 mL of 100 mM phosphate buffer (pH 7.0) APF or 3 μM HPF and 300 μM FAS plus, where specified, 1 mM NaN_3 or 1% DMSO. After a stable base-line was established (excitation = 492 nm, emission = 525 nm), H_2O_2 was added (300 μM) and the increase in fluorescence was monitored over 120 s, by which time there was no further change. Data represent the mean ± SD for three determinations, and represent fluorescence (in arbitrary units) above the base-line level.

Table 2

Morphometric analysis.

Conditions	Average gray value	%
Control	3.8 ± 2.4	6.5
BPD	58.5 ± 16.3	100*
BPD + 1% DMSO	32.8 ± 10.3	56
BPD + 100 μM DFO	32.5 ± 5.8	56
BPD + both	28.7 ± 14.5	49
BPD + 0.1% DMSO	49.7 ± 7.2	85

These figures represent a morphometric analysis (mean ± SD) of images shown in Fig. 4 (see text).

* These data are calculated in terms of the percentage of the mean value for the average gray value for the “BPD” sample.